Journal of Glaciology, Vol. 44, No. 147, 1998

Instruments and methods

Inter-borehole electrical resistivity imaging of englacial drainage

Bryn Hubbard,[1] Andrew Binley,[2] Lee Slater,[2*] Roy Middleton,[2] Bernd Kulessa[1]
[1]*Centre for Glaciology, Institute of Geography and Earth Sciences, University of Wales, Aberystwyth, Ceredigion SY23 3DB, Wales*
[2]*Department of Environmental Science, Institute of Environmental and Natural Sciences, Lancaster University, Lancaster, Lancashire LA1 4YQ, England*

ABSTRACT. Borehole-based electrical resistivity surveys have the capacity to enhance our understanding of the structure of englacial drainage pathways in temperate ice. We summarize inter-borehole electrical resistivity tomography (ERT) as currently used in hydrogeological investigations and as adapted for imaging englacial drainage. ERT connections were successfully made for the first time in glacier ice, following artificial mineralization of borehole waters at Haut Glacier d'Arolla, Switzerland. Here, two types of electrical connection were made between boreholes spaced up to 10 m apart and drilled to depths of between 20 and 60 m. Most tests indicated the presence of resistively homogeneous ice with uniform bulk resistivities of $\sim 10^8$–$10^9\ \Omega$ m. However, ERT was also successfully used to identify and characterize a hydraulically conductive englacial fracture that intersected two boreholes at a depth of ~13 m below the glacier surface. The presence of this connecting void was suggested by drilling records and verified by dual borehole-impulse testing. The reconstructed tomogram for these boreholes is characterized by a background ice-resistivity field of $\sim 10^9\ \Omega$ m that is disrupted at a depth of ~13 m by a sharp, sub-horizontal low-resistivity zone ($\sim 10^4\ \Omega$ m). Inter-borehole ERT, therefore, has the capacity to image both uniform and fractured temperate glacier ice.

INTRODUCTION

The flow pathways by which surface-generated meltwaters are routed through temperate glaciers are poorly understood. It is generally accepted that such drainage takes one of two broad forms, depending on the manner in which the water enters the glacier. First, meltwaters introduced via crevasses or moulins are inferred, principally from dye-return times, to flow rapidly along large conduits to the glacier bed (e.g. Behrens and others, 1971). Direct exploration of moulins indicates that they descend approximately vertically for some tens of metres before deviating laterally and becoming constricted, thereby preventing further exploration (e.g. Holmlund, 1988). Sudden deviations of this kind, however, may not be universal. Comparison of cable length with water depth in moulins on White Glacier, Canadian Arctic, indicates gradual deviation from the vertical with depth (Iken, 1972). Similarly, Hooke (1984) argued that where englacial conduits are only partially water-filled, they should develop a near-vertical orientation, particularly deeper in the ice, as a result of melting being focused on their lowermost ice boundaries. Secondly, meltwater may permeate ice via intergranular veins (Nye and Frank, 1973), which may coalesce with depth to form progressively larger and more effective capillary-sized tubes (Nye, 1989). However, the actual intergranular permeability of temperate ice is poorly known, having been addressed by only a small number of studies (e.g. Lliboutry, 1971, 1996; Wakahama and others, 1973; Raymond and Harrison, 1975; Berner and others, 1977; Hantz and Lliboutry, 1983). The issue of whether supraglacial and englacial meltwaters can aggregate within ice to form tubes that might evolve with depth into an arborescent network of larger conduits is even more difficult to assess. While Lliboutry (1971) argued against such a development, veinlets some millimetres in diameter were observed in ice cores recovered from a depth of ~20 m in Blue Glacier, U.S.A. (Raymond and Harrison, 1975), whereas decimetre-size englacial voids are now commonly identified by borehole video (Pohjola, 1994; Harper and Humphrey, 1995; Copland and others, 1996). The orientation of these larger flow pathways (including those draining moulins and crevasses), however, is poorly understood, although they are commonly assumed to be aligned orthogonal to the inferred local hydraulic pressure gradient (Shreve, 1972; cf. Hooke, 1984).

Our current understanding of englacial drainage in temperate glaciers is therefore in need of empirical clarification. Electrical resistivity tomography (ERT) represents a potential means of providing such information, since the technique enables one to reconstruct the internal resistivity distribution of a medium from multiple resistance measurements made at its boundaries (Fig. 1). In addition to applications in the fields of medical research (as "electrical impedance tomography") (e.g. Webster, 1990) and the process industry (e.g. Dickin and Wang, 1996), hydrogeological applications have focused principally on borehole-based re-

* Present address: Department of Geosciences, University of Southern Maine, Gorham, Maine 04038, U.S.A.

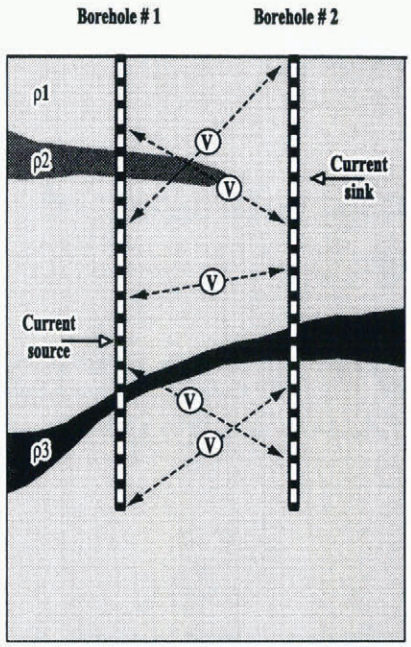

Fig. 1. Inter-borehole ERT electrode geometry for the determination of bulk material resistivities ρ1, ρ2 and ρ3. Black squares represent electrodes. Note that, since borehole waters are artificially mineralized in the present case, current is injected and voltage measured only between the boreholes.

constructions of sub-surface patterns of ground water, tracer or contaminant flow (e.g. Daily and Owen, 1992; Ramirez and others, 1996). Significantly, the resulting resistivity fields, or *tomograms*, are created without physically disturbing the host material concerned. The technique should therefore be well suited to reconstructing englacial drainage patterns, since temporal or spatial variability in the drainage character may be accompanied by closely related resistivity variations.

In this paper, we describe the theory, apparatus and methods used in applying ERT to investigating in situ the structure of englacial drainage in temperate glaciers. Preliminary results are reported from Haut Glacier d'Arolla, Switzerland, where two types of inter-borehole ERT connection have been recorded.

THEORY, APPARATUS AND METHODS

Inter-borehole electrical resistivity tomography (ERT)

Inter-borehole ERT involves sequentially exciting and recording potential differences across multiple electrode pairs located down boreholes in order to determine the resistivity field of the intervening space (Fig. 1). Each linearly independent pairing of drive and response electrodes is sequentially interchanged, providing a large number of combinations of independent transfer resistances between electrode strings. The resulting data are transformed into resistivity tomograms via inverse numerical methods, which compute an optimum set of effective resistivity values in the intervening space.

Forward modelling

The forward model is the solution of the electrical potential field due to an applied electrical current in a region of specified resistivity distribution. For two-dimensional investigations, the forward model is the Fourier transformed Poisson's equation:

$$\frac{\partial}{\partial x}\left(\frac{1}{\rho}\frac{\partial v}{\partial x}\right)+\frac{\partial}{\partial z}\left(\frac{1}{\rho}\frac{\partial v}{\partial z}\right)\lambda^2\frac{v}{\rho}=-I\delta(x)\delta(z) \qquad (1)$$

where v is electrical potential, x and z are Cartesian coordinates, ρ is resistivity, I is applied current, λ is the Fourier transform variable and $\partial(x)$ and $\partial(z)$ are delta functions. By using the Fourier transformation, we are able to simulate three-dimensional current flow, although the resistivity distribution is assumed to be two-dimensional. The model is computed on a finite-element mesh with elements extending to some considerable distance away from the electrodes to account for infinite current-flow boundaries. Uniform resistivity is assumed within each finite element.

Inverse modelling

Inversion is based on the Occam's approach of deGroot–Hedlin and Constable (1990), similar to that described in some detail by Morelli and others (1996). Here, the region of interest is parameterized using a finite-element mesh, the resistivity of which is determined by the inverse model. The solution is based on the minimization of the objective function:

$$\Phi(m)=[D-F(m)]^T\mathbf{W}^{-1}[D-F(m)]+\alpha m^T R m \qquad (2)$$

where $m=\log_e(\rho^{-1})$, D are the measured resistances, $F(m)$ are the corresponding forward model resistances due to parameters m, $\mathbf{W}$ is a vector of data variances used to weight individual measurements, R is a roughness matrix used to force smoothing of the resistivity distribution and to stabilize the inverse solution, and α is a smoothing parameter. Minimization of the objective function in Equation (2) is achieved through an iterative solution, the procedure terminating when data misfit has been reduced to the desired level.

Data errors

Experience has shown that characterization of data errors is critical for successful inverse solutions of ERT data. These data errors permit the weighting of measurements through the vector, $\mathbf{W}$, in Equation (2). Errors are characterized according to measurement repeatability and reciprocity. However, measurements may frequently repeat but not reciprocate to the same degree. We therefore utilize a strict characterization of data errors by collecting reciprocal equivalents of all measurements (see Binley and others, 1995). In the present study, measurements with reciprocal errors greater than 5% are removed prior to inversion. Inversion of a single dataset typically takes 30 min on a Pentium 200 MHz PC.

Adaptation for englacial investigations

The application of ERT to investigating englacial hydrology requires (i) that bulk material resistivities are low enough to permit the establishment of an electrical circuit between boreholes, and (ii) that there is a detectable resistivity contrast between the host glacier ice and the englacial water being imaged. These requirements, however, are unlikely in the englacial zone of temperate glaciers, since bulk glacier ice and englacial waters have resistivities that are typically greater than 10^6 and $10^4\,\Omega$ m, respectively. This resistivity contrast, however, may be enhanced by artificially mineralizing borehole waters through the addition of a saline (NaCl) solution. Such mineralization, however, has the

https://doi.org/10.3189/S0022143000002756 Published online by Cambridge University Press

effect of channelling current preferentially along boreholes rather than across them. In order to combat this effect, the measurement schedule adopted in the present study defines only configurations that locate current and potential electrode pairs in separate boreholes (see Fig. 1). Since such a schedule records only borehole-to-borehole electrical current flow, only flow pathways of this orientation are identified. Slater and others (1997) successfully applied such a technique in mapping the distribution of hydraulically conductive conduits in a limestone aquifer. In cases where distinct hydraulic (and hence electrical) connections do not exist between boreholes, however, a significant amount of current will flow through the relatively conductive borehole fluid. Boreholes will, in fact, act as line electrode sources in such situations, despite the adopted measurement scheme. The present study, however, is principally concerned with identifying situations where significant electrical current flow is channelled through water-filled, inter-borehole connections. Such configurations should present inter-borehole pathways that are sufficiently electrically conductive to be imaged. In addition, the adopted assumption of two-dimensional resistivity variation is not truly appropriate here given the electrical conductivity contrasts caused by the borehole fluid. The three-dimensional nature of the current flow could be accounted for by changes to the forward-modelling scheme but, given the excessive computational burden caused by this, we have decided to maintain the assumption of two-dimensional variation in resistivity.

Apparatus

The data-acquisition system used in the present study is based on a single-channel, Geopulse resistance meter (manufactured by "Campus Geophysical Instruments Ltd, UK") incorporating both transmitting and receiving units (Fig. 2). The transmitter was powered by two external 24 Ah, 12 V batteries that were rotated daily between operation and recharge by an 8 W solar panel. The transmitter generates a mechanically reversed d.c. signal (thereby preventing electrode polarization) which can be selected in steps between 0.1 and 100 mA to a maximum power output of 18 W. The receiver incorporates automatic gain steps which provide a range of measurements from 1 to $2 \times 10^6\ \Omega$, revealed by calibration checks against known resistors to be accurate to better than 1% (personal communication from S. Binns, 1996). Geopulse signal transmission and data acquisition are automated via PC-compatible software supplied by the manufacturer. A 64-port multiplexer is used to provide automatic switching between electrode configurations. For each transfer-resistance measurement, the current and potential source/sink electrodes are specified. Borehole electrodes were composed of lead strips (~3 mm thick and 4 cm wide) wrapped once around, and taped at their edges to 5 cm diameter, 20 m long PVC pipe. Each electrode was soldered to a length of single-core, multi-strand cable which travelled up the interior of the pipe to the multiplexer located at the glacier surface (Fig. 2). Borehole ERT data were collected using these 20 m long sections. ERT investigations in the field are, in the main, constrained by portability (dictated principally by the electrode arrays) and the environmental requirements for PC operation.

Boreholes were drilled using the pressurized, hot-water system ("Kärcher HDS-100") described elsewhere (Hubbard and others, 1995). In order to replace borehole water with saline water, 0.2 kg of table salt was mixed with 200 l of supraglacial water in a water butt (normally used as a constant-head water supply) and the drill was used to pump this water, unheated, into the borehole. A large-diameter reaming tip (used to reduce water pressure to ~30 bar at the point of delivery) was used for this process. A uniform salinity distribution was induced by raising and lowering the drill stem along the borehole during pumping.

Field site and experiments

Field experiments were conducted in August 1996 and August 1997 in the ablation area of Haut Glacier d'Arolla, Switzerland (Fig. 3). This 6.3 km^2, temperate valley glacier extends from ~2560 m a.s.l. at its snout to ~3500 m a.s.l. at its headwall. The morphology, dynamics, hydrology and hydrochemistry of this glacier have been intensively investigated over the past decade, and have been described elsewhere (e.g. Sharp and others, 1993; Hubbard and others, 1995; Richards and others, 1996; Harbor and others, 1997). Resistance measurements were made between numerous pairs of boreholes drilled to terminate englacially at depths of ~60 m (1996) or ~20 m (1997) in an area close to the eastern margin of the glacier, where the ice is ~100 m thick (Fig. 3).

The utility of these techniques to investigations of englacial hydrology may be illustrated by two ERT-response patterns obtained during the field experiments.

RESULTS

Inter-borehole ERT in homogeneous ice

Most inter-borehole ERT experiments conducted in this study indicate highly resistive, uniform formations. This

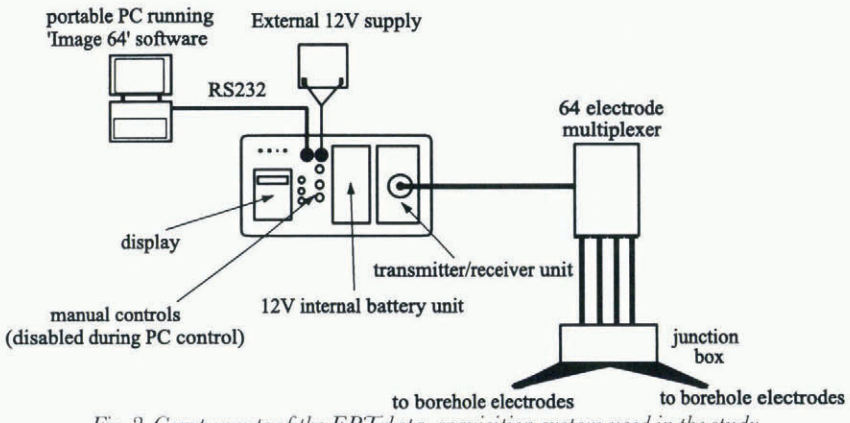

Fig. 2. Components of the ERT data-acquisition system used in the study.

https://doi.org/10.3189/S0022143000002756 Published online by Cambridge University Press

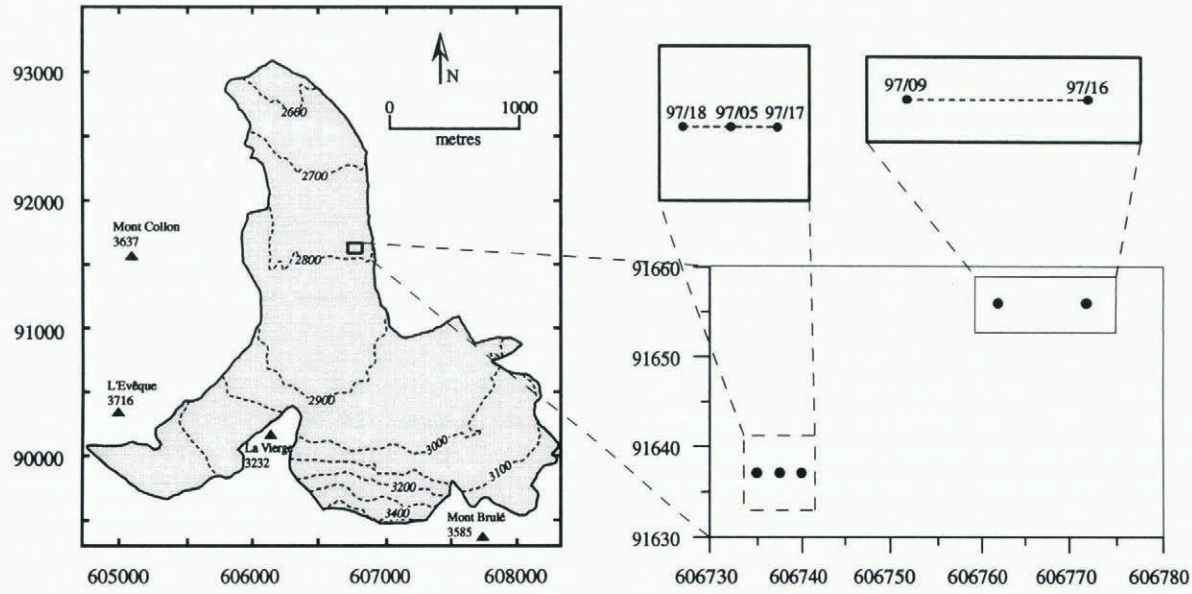

Fig. 3. Haut Glacier d'Arolla, Switzerland, with locations of selected boreholes. Locations of inter-borehole tomograms referred to in the text and reproduced in Figures 4 and 6 are shown by dashed lines.

pattern is readily illustrated by the reconstructed resistivity field between boreholes 97–09 and 97–16 (Fig. 4). These 20 m deep boreholes are selected because they are separated by a greater distance (10 m) than any of the other tested boreholes. The resulting tomogram is visually similar to all others conducted in homogeneous ice, including experiments conducted in more closely spaced but deeper (60 m), 1996 boreholes. The 97–09 to 97–16 tomogram is characterized by resistivities that are uniform in the vertical plane and which increase gradually in the horizontal, englacial plane from the centre of each borehole to the midpoint separating them. We interpret the vertically uniform resistivity pattern in terms of the general absence of macroporous preferential flow pathways between the boreholes; an inference that is supported by the absence of spatially coincident englacial voids noted during drilling. Significantly, similar homogeneous images have been obtained within massive limestone formations where no preferential current channel existed between boreholes (Slater and others, 1997). We interpret the increasing resistivity away from the boreholes in the horizontal plane in terms of three, largely processing-based effects. First, as noted above, the two-dimensional inversion used in this analysis assumes uniform resistivities orthogonal to the image plane. In reality, this assumption is violated by the three-dimensional expression of the saline borehole, inducing artificially low resistivities adjacent to the boreholes in the image plane. Secondly, due to the high resistivity of the inter- borehole region relative to the borehole fluid, a significant amount of current flows along the length of the borehole, artificially decreasing near-borehole resistivities. Thirdly, the penalty function being used does not allow strong resistivity gradients between adjacent cells, in this case producing an artificially weak gradient away from the boreholes. However, the generation of consistent resistivities (of $\sim 10^8$–$10^9\,\Omega\,m$) along the centre of the image that are substantially higher than those capable of being recorded by the apparatus, suggests that this value does represent the actual resistivity of the ice being imaged. Significantly, 10^8–$10^9\,\Omega\,m$ is consistent with (though at the upper range of) previous, surface-based, estimates of the resistivity of temperate glacier ice (e.g. Röthlisberger, 1967; Röthlisberger and Vögtli, 1967).

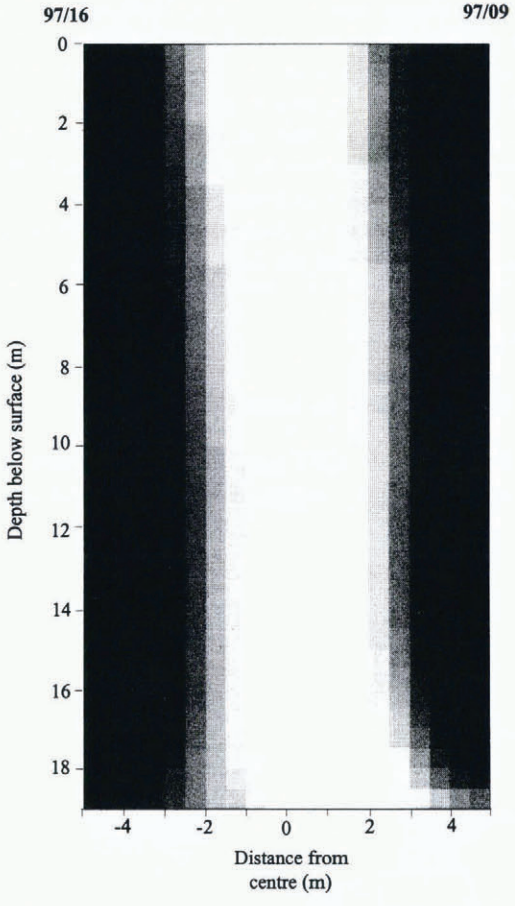

Fig. 4. Tomogram recorded between boreholes 97–09 and 97–16 (20 m deep; 10 m apart).

ERT between boreholes intersected by a hydraulically conductive fracture

A small englacial void was intersected at a depth of ~13 m during the drilling of boreholes 97–05, 97–17 and 97–18. In each case, the drill stem free-fell some centimetres at this depth, although the water levels within the boreholes remained within some decimetres of the ice surface. That these boreholes were hydraulically connected at depth was indi-

https://doi.org/10.3189/S0022143000002756 Published online by Cambridge University Press

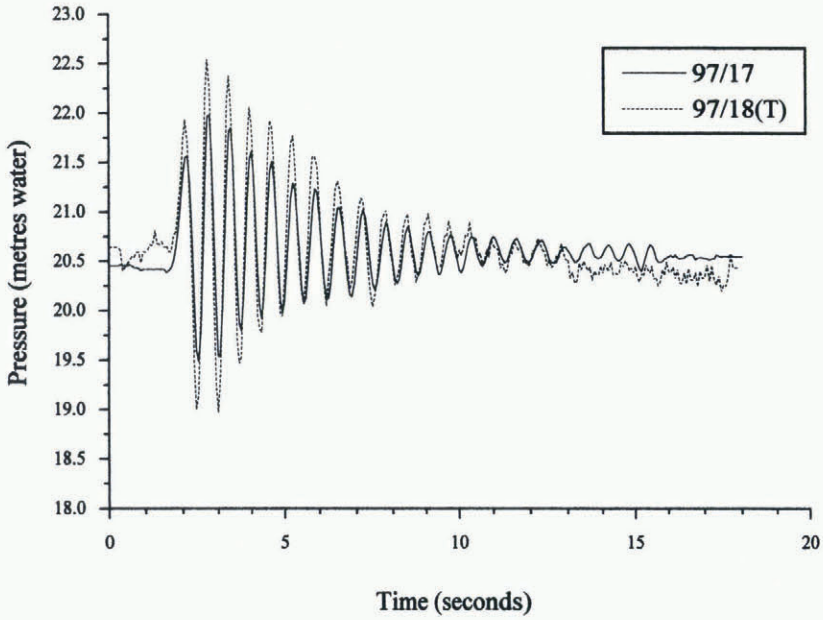

Fig. 5. Impulse test water-pressure response oscillations recorded simultaneously in boreholes 97–17 and 97–18. The impulse load was introduced only into borehole 97–18, indicating a hydraulic connection between the boreholes. "T" indicates borehole containing signal source.

cated by fluctuations in their water levels as each newly drilled borehole connected with the englacial void (boreholes were drilled in chronological order 97–05, 97–17 and 97–18). For example, the water level in borehole 97–17 fell some centimetres immediately upon connection with the void at ~13 m, and water was simultaneously forced out from the top of borehole 97–05. Both water levels then fluctuated in apparent anti-phase as drilling continued to the base of 97–17. Similar events characterized the drilling of 97–18. A series of paired impulse tests was carried out between these boreholes in order to verify more rigorously the presence of a hydraulic connection between them. To date, single borehole impulse tests have been carried out in ice principally to investigate the nature of the basal drainage system to which the boreholes are connected (e.g. Stone and Clarke, 1993; Iken and others, 1996; Kulessa and Hubbard, 1997). In the present case, however, we recorded pressure simultaneously (at 16 Hz) in both boreholes 97–17 and 97–18 while only the latter was slug-loaded. Significantly, this test resulted in similar pressure-response oscillations being recorded in both boreholes (Fig. 5). This response contrasts with earlier paired impulse tests at closely spaced (but apparently unconnected) boreholes in the glacier, where non-tested boreholes showed no measurable response (Kulessa and Hubbard, 1997). We therefore infer from both borehole drilling and impulse-testing records that boreholes 97–05, 97–17 and 97–18 are hydraulically connected, probably by a small englacial flow pathway located at a depth of about 13 m.

ERT experiments were carried out between boreholes 97–17 and 97–18 with the intention of identifying and characterizing this englacial connection. For this purpose, both boreholes 97–17 and 97–18 were mineralized, while 97–05 was left filled with high-resistivity supraglacial (drill) water. The resulting tomogram (Fig. 6) differs markedly from any other acquired in the study. A sub-horizontal zone of anomalously low resistivity is clearly identified between the depths of 12.5 and 14 m, coincident with the inferred fracture or channel. The lowest resistivities in this zone ($\sim 10^4\ \Omega$ m) are recorded in what appears to be a chamber located 1–2 m west of the edge of borehole 97–17 (Fig. 3). The low-resistivity

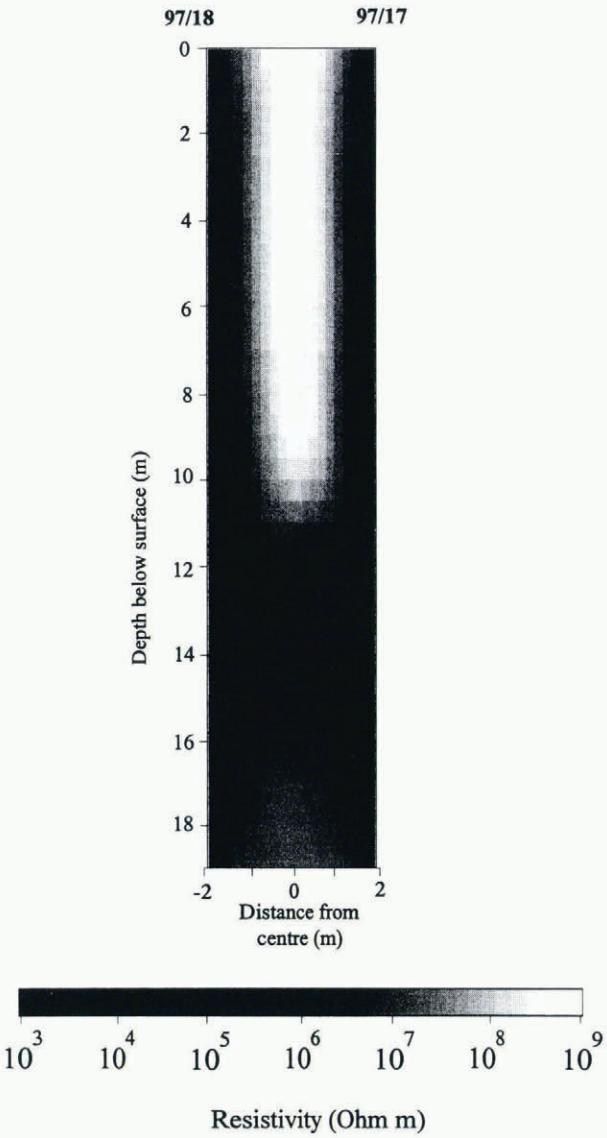

Fig. 6. Tomogram recorded between boreholes 97–17 and 97–18. The presence of a hydraulically conductive fracture, suspected on the basis of drilling and dual impulse-test records (see Fig. 5), is apparant as a low-resistivity zone at a depth of ~13 m.

https://doi.org/10.3189/S0022143000002756 Published online by Cambridge University Press

zone also appears to intersect both boreholes, as expected, at a depth of ~13 m. In contrast to this low-resistivity zone, the rest of the tomogram is similar to those recorded in resistively uniform ice (Fig. 4), indicating the absence of other, hydraulically conductive fractures.

SUMMARY

Electrical resistivity tomography can provide useful information relating to the hydraulic structure of englacial ice. The technique, which is used increasingly in hydrogeophysical investigations, should appeal to glaciologists, because it does not disturb the structure of the ice under examination. In contrast to ground-water investigations, however, surveys of englacial drainage pathways require mineralization of the current-bearing meltwaters and commensurate alteration of the measurement schedule, in order to avoid the dominance of along-borehole conductivity pathways. Application of cross-borehole ERT in the ablation area of Haut Glacier d'Arolla, Switzerland, has successfully resulted in the first tomograms of glacier ice. Analysis of these indicates at least two hydraulic configurations may be identified:

1. Hydraulically homogeneous ice containing only micro-porous flow pathways is characterized by vertically uniform tomograms that indicate ice resistivities of 10^8–$10^9\ \Omega$ m.

2. Discrete, hydraulically conductive flow pathways may be identified and imaged as low-resistivity zones that disrupt the background high-resistivity field.

Both results provide encouragement for the application of more extensive ERT investigations in the future.

ACKNOWLEDGEMENTS

This work was supported by a U.K. NERC research grant (GR9/2530). We wish to thank A. Watson, C. Acton, B. Rule and Y. Bams for assistance in the field, and R. Hooke, J. Kohler and an anonymous referee for helpful comments on an earlier version of the manuscript.

REFERENCES

Behrens, H. *and 7 others*. 1971. Study of the discharge of alpine glaciers by means of environmnetal isotopes and dye tracers. *Z. Gletscherkd. Glazialgeol.*, **7**(1–2), 79–102.

Berner, W., B. Stauffer and H. Oeschger. 1978. Dynamic glacier flow model and the production of internal meltwater. *Z. Gletscherkd. Glazialgeol.*, **13**(1–2), 1977, 209–217.

Binley, A., A. Ramirez and W. Daily. 1995. Regularised image reconstruction of noisy electrical resistance tomography data. *In* Beck, M. S., B. S. Hoyle, M. A. Morris, R. C. Waterfall and R. A. Williams, *eds. Process tomography 1995.* Manchester, UMIST, 401–410.

Copland, L., J. Harbor, S. Gordon and M. Sharp. 1996. The use of borehole video in investigating the hydrology of a temperate glacier. *Hydrol. Processes*, **11**(2), 211–224.

Daily, W., A. Ramirez, D. LaBrecque and J. Nitao. 1992. Electrical resistivity tomography of vadose water movement. *Water Resour. Res.*, **28**(5), 1429–1442.

deGroot-Hedlin, C. and S. Constable. 1990. Occam's inversion to generate smooth, two-dimensional models from magnetotelluric data. *Geophysics*, **55**(12), 1613–1624.

Dickin, F. and M. Wang. 1996. Electrical resistance tomography for process applications. *Measurement Science and Technology*, **7**(3), 247–260.

Hantz, D. and L. Lliboutry. 1983. Waterways, ice permeability at depth, and water pressures at Glacier d'Argentière, French Alps. *J. Glaciol.*, **29**(102), 227–239.

Harbor, J., M. Sharp, L. Copland, B. Hubbard, P. Nienow and D. Mair. 1997. The influence of subglacial drainage conditions on the velocity distribution within a glacier cross section. *Geology*, **25**(8), 739–742.

Harper, J.T. and N. F. Humphrey. 1995. Borehole video analysis of a temperate glacier's englacial and subglacial structure: implications for glacier flow models. *Geology*, **23**(10), 901–904.

Holmlund, P. 1988. Internal geometry and evolution of moulins, Storglaciären, Sweden. *J. Glaciol.*, **34**(117), 242–248.

Hooke, R. LeB. 1984. On the role of mechanical energy in maintaining subglacial water conduits at atmospheric pressure. *J. Glaciol.*, **30**(105), 180–187.

Hubbard, B. P., M. J. Sharp, I. C. Willis, M. K. Nielsen and C. C. Smart. 1995. Borehole water-level variations and the structure of the subglacial hydrological system of Haut Glacier d'Arolla, Valais, Switzerland. *J. Glaciol.*, **41**(139), 572–583.

Iken, A. 1972. Measurements of water pressure in moulins as part of a movement study of the White Glacier, Axel Heiberg Island, Northwest Territories, Canada. *J. Glaciol.*, **11**(61), 53–58.

Iken, A., K. Fabri and M. Funk. 1996. Water storage and subglacial drainage conditions inferred from borehole measurements on Gornergletscher, Valais, Switzerland. *J. Glaciol.*, **42**(141), 233–248.

Kulessa, B. and B. Hubbard. 1997. Interpretation of borehole impulse tests at Haut Glacier d'Arolla, Switzerland. *Ann. Glaciol.*, **24**, 397–402.

Lliboutry, L. 1971. Permeability, brine content and temperature of temperate ice. *J. Glaciol.*, **10**(58), 15–29.

Lliboutry, L. 1996. Temperate ice permeability, stability of water veins and percolation of internal meltwater. *J. Glaciol.*, **42**(141), 201–211.

Morelli, G. and D. J. LaBrecque. 1996. Robust scheme for ERT inverse modelling. *In SAGEEP 96, Symposium on Application of Geophysics to Engineering and Environmental Problems, April 28 – May 2, 1996, Keystone, Colorado.* Wheat Ridge, CO, U.S.A., Environmental and Engineering Geophysical Society, 629–638.

Nye, J. F. 1989. The geometry of water veins and nodes in polycrystalline ice. *J. Glaciol.*, **35**(119), 17–22.

Nye, J. F. and F. C. Frank. 1973. Hydrology of the intergranular veins in a temperate glacier. *International Association of Scientific Hydrology Publication* 95 (Symposium at Cambridge 1969 — *Hydrology of Glaciers*), 157–161.

Pohjola, V. A. 1994. TV-video observations of englacial voids in Storglaciären, Sweden. *J. Glaciol.*, **40**(135), 231–240.

Ramirez, A., W. Daily, A. Binley, D. LaBrecque and D. Roelant. 1996. Detection of leaks in underground storage tanks using electrical resistance methods. *Journal of Environmental Engineering Geophysics*, **1**(3), 189–203.

Raymond, C. F. and W. D. Harrison. 1975. Some observations on the behavior of the liquid and gas phases in temperate glacier ice. *J. Glaciol.*, **14**(71), 213–233.

Richards, K. S. *and 9 others*. 1996. An integrated approach to modelling hydrology and water quality in glacierized catchments. *Hydrol. Processes*, **10**(4), 479–508.

Röthlisberger, H. 1967. Electrical resistivity measurements and soundings on glaciers: introductory remarks. *J. Glaciol.*, **6**(47), 599–606.

Röthlisberger, H. and K. Vögtli. 1967. Recent D.C. resistivity soundings on Swiss glaciers. *J. Glaciol.*, **6**(47), 607–621.

Sharp, M. J. *and 6 others*. 1993. Geometry, bed topography and drainage system structure of the Haut Glacier d'Arolla, Switzerland. *Earth Surface Processes and Landforms*, **18**(6), 557–571.

Shreve, R. L. 1972. Movement of water in glaciers. *J. Glaciol.*, **11**(62), 205–214.

Slater, L. D., A. Binley and D. Brown. 1997. Electrical imaging of fractures using ground-water salinity change. *Ground Water*, **35**(3), 436–442.

Stone, D. B. and G. K. C. Clarke. 1993. Estimation of subglacial hydraulic properties from induced changes in basal water pressure: a theoretical framework for borehole-response tests. *J. Glaciol.*, **39**(132), 327–340.

Wakahama, G. *and 6 others*. 1973. [Observations of permeating water through a glacier body.] *Low Temp. Sci., Ser. A* 31, 209–219. [In Japanese with English summary.]

Webster, J.G. 1990. *Electrical impedance tomography*. Bristol, Adam Hilger.

MS received 14 July 1997 and accepted in revised form 1 February 1998